SAGE-Hindawi Access to Research
Journal of Dental Biomechanics
Volume 2011, Article ID 752741, 10 pages
doi:10.4061/2011/752741

*Research Article*

# A Qualitative Engineering Analysis of Occlusion Effects on Mandibular Fracture Repair Mechanics

**Thomas R. Katona**

*Indiana University School of Dentistry, Indiana University—Purdue University, Indianapolis (IUPUI), 1121 W. Michigan Street, Indianapolis, IN 46202, USA*

Correspondence should be addressed to Thomas R. Katona, tkatona@iupui.edu

Received 5 May 2011; Revised 30 June 2011; Accepted 22 August 2011

Academic Editor: Jan Harm Koolstra

Copyright © 2011 Thomas R. Katona. This is an open access article distributed under the Creative Commons Attribution License, which permits unrestricted use, distribution, and reproduction in any medium, provided the original work is properly cited.

*Objectives*. The purpose of this analytical study was to examine and critique the engineering foundations of commonly accepted biomechanical principles of mandible fracture repair. *Materials and Methods*. Basic principles of static equilibrium were applied to intact and plated mandibles, but instead of the traditional lever forces, the mandibles were subjected to more realistic occlusal forces. *Results*. These loading conditions produced stress distributions within the intact mandible that were very different and more complex than the customary lever-based gradient. The analyses also demonstrated the entirely different mechanical environments within intact and plated mandibles. *Conclusions*. Because the loading and geometry of the lever-idealized mandible is incomplete, the associated widely accepted bone stress distribution (tension on top and compression on the bottom) should not be assumed. Furthermore, the stress gradients within the bone of an intact mandible should not be extrapolated to the mechanical environment within the plated regions of a fractured mandible.

## 1. Introduction

The mandible has long been regarded as a lever [1–13]. There have been questions about its class I versus II versus III classification, or it being a lever in the first place [14–16] and the loading assumptions [17]. But it is the lever model, coupled with the bending beam analogy of the mandible that form the foundation of the generally accepted (longitudinal) stress distribution pattern depicted in Figure 1(a) [18–21] and its variant, Figure 1(b) [18, 20, 22, 23].

The lever is an oversimplified structural representation of the jaw, so biomechanical concepts derived from it should be suspect. In the present context, the lever's intrinsic vertical-only occlusal force is its primary drawback. Thus, the principal purposes of this paper are to demonstrate, with basic analytical engineering mechanics, but barebones mathematics, the shortcomings of the lever/beam model-based concepts that relate to the surgery of the mandible. More specifically, the central issues involve (1) the relationship between occlusal force direction and the associated stress distributions within an intact mandible and (2) the extrapolation of those stress fields to a plated fractured mandible.

## 2. Materials and Methods

Figure 2(a) is a partial (because dimensions irrelevant to this discussion are omitted) free-body diagram (FBD) of the frame- (versus lever-, Figure 1) idealized mandible. An FBD, used in equilibrium analysis, shows all external loads (forces and moments) that act on an isolated object (i.e., the mandible or a portion of it) of interest. For the purposes of this project, the crucial difference between the lever (Figure 1) and the frame model is that in the latter, the direction of force vector **T** is not necessarily vertical, Figures 2 and 3. (The governing equations for Figure 2(a) are derived and solved elsewhere [24].)

The FBD in Figure 2(b) is of an imaginary or real (i.e., fractured) segment of the mandible that is anterior to the arbitrarily defined (at distance $h$ from the occlusal contact) circle, ◯, on the approximated centroidal axis (dashed line) of the mandible. $\mathcal{V}$ and $\mathcal{H}$ represent the internal shear and normal (perpendicular) forces, respectively, and $\mathcal{M}$ represents the internal moment. $\mathcal{V}$, $\mathcal{H}$, and $\mathcal{M}$ symbolize the net internal loads at the interface (real or imaginary) that are necessary to maintain the static equilibrium of the anterior

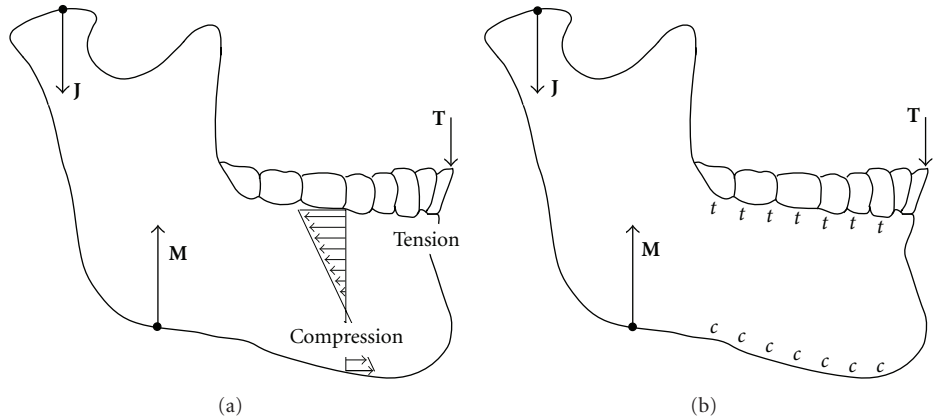


FIGURE 1: (a) The typical representation of the lever-based tension on top/compression on bottom (tot/cob) stress distribution within the mandible. (**J**, **M,** and **T** are the joint, muscle, and occlusal forces, respectively.) (b) a variant depiction of tot/cob.

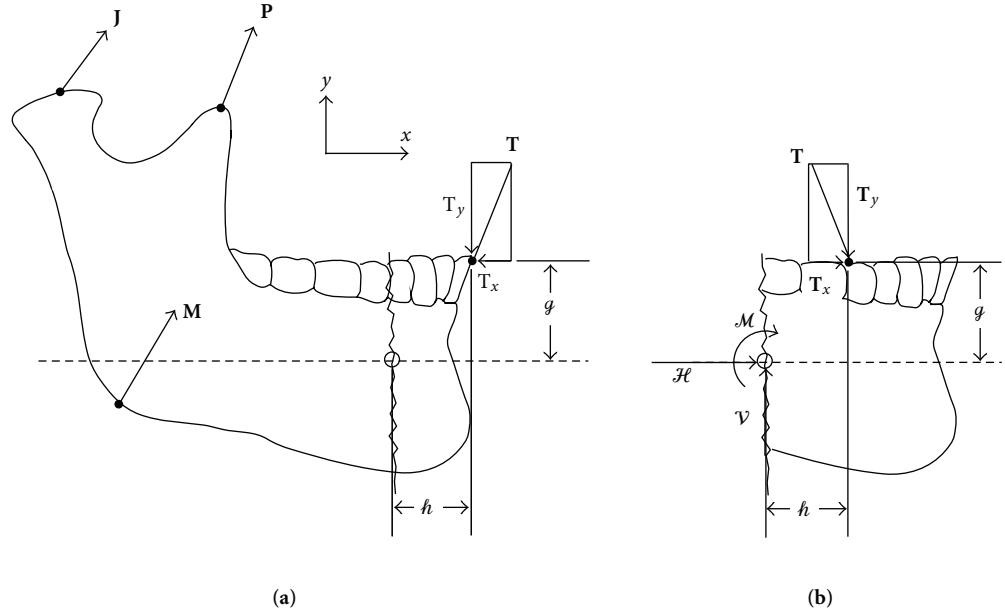


FIGURE 2: (a) Nonlever model of the mandible illustrating a generic tooth contact, adapted from Katona [24]. The approximation to the centroidal (neutral) axis of the mandible (dashed line) is a distance $g$ below the tooth-tooth contact point. The anterior section of interest is demarcated by horizontal distance $h$ from the tooth contact. (b) FBD (free-body diagram) of the (fractured-off or imaginary) anterior segment.

segment when occlusal force **T** acts on it. Applying static equilibrium conditions to the FBD in Figure 2(b) yields

$$\sum \text{Forces}_{\text{vertical}} = 0 : \mathcal{V} - T_y = 0 \quad \text{or} \quad \mathcal{V} = T_y,$$

$$\sum \text{Forces}_{\text{horizontal}} = 0 : \mathcal{H} + T_x = 0 \quad \text{or} \quad \mathcal{H} = -T_x,$$

$$\sum \text{Moments about}_{\text{o}} = 0 : -\mathcal{M} - hT_y - gT_x = 0$$

$$\text{or} \quad \mathcal{M} = -hT_y - gT_x. \tag{1}$$

The right hand sides of the equations are known because they are specified or calculated. For the purposes of this project, it is important only to recognize that $\mathcal{V}$ and $\mathcal{H}$ are determined by $T_y$ and $T_x$, respectively, and that $\mathcal{M}$ is a function of both $T_y$ and $T_x$, as well as anatomy ($g$) and the horizontal distance ($h$) between the section and the occlusal contact.

The analysis is based on the range of occlusal force directions represented in Figure 3(a). Three contact configurations are possible between opposing teeth. Occlusal contact can occur between a maxillary cusp distal incline and a mandibular cusp mesial incline ($\mathbf{T}_0$, $\mathbf{T}_1$, and $\mathbf{T}_2$), a maxillary cusp mesial incline against a mandibular cusp distal incline ($\mathbf{T}_4$) or flat-plane occlusion ($\mathbf{T}_3$, also in Figure 1). (According to classic friction principles, assuming frictionless contact, the direction of a contact force between surfaces must be perpendicular to their common tangent. The qualitative outcomes presented herein would not be affected by friction [25].)

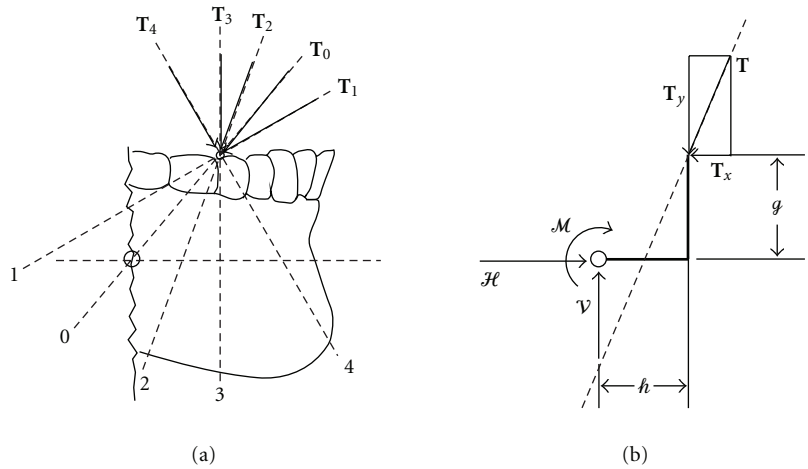


FIGURE 3: (a) The 5 mechanically distinctive orientations of **T** defined by relative location ($g$ and $h$, Figure 2(b)) and cusp contact inclination. $\mathbf{T}_1$, $\mathbf{T}_0$, and $\mathbf{T}_2$ have posteriorly directed horizontal components. $\mathbf{T}_3$ is vertical. $\mathbf{T}_4$ has an anterior component. $\mathbf{T}_1$ produces a ccw moment about the circle. $\mathbf{T}_0$ generates no moment. $\mathbf{T}_2$, $\mathbf{T}_3$, and $\mathbf{T}_4$ generate cw moments. (b) A generic representation of Figures 2(b) and 3(a). Note that a change in the anterior-posterior relative location of bite contact and ◯ is defined by $h$. Occlusal plane height is given by $g$.

$\mathbf{T}_{0\text{--}4}$ can be characterized by the positions of their lines-of-action (LOA) relative to the circle, ◯. $\mathbf{T}_1$ passes above (or equivalently, behind) it, thus requiring a clockwise (cw) moment, $-\mathcal{M}$, for equilibrium. $\mathbf{T}_0$ passes through it, therefore $\mathcal{M} = 0$. Equilibrium dictates that $\mathcal{M}$ must be counterclockwise (ccw) with $\mathbf{T}_2$, $\mathbf{T}_3$, and $\mathbf{T}_4$, because they pass below or in front of ◯.

The second relevant characteristic of a **T** is the direction of its horizontal component. $\mathbf{T}_0$, $\mathbf{T}_1$, and $\mathbf{T}_2$ are directed posteriorly; therefore, for equilibrium, $\mathcal{H}$ must be to the right. Because $\mathbf{T}_3$ (the lever analogue) is vertical, $\mathcal{H} = 0$. The forward component of $\mathbf{T}_4$ requires that $\mathcal{H}$ must be to the left. Thus, the 5 **T**s generically represent the permutations of the LOA orientations relative to ◯ and the horizontal force component directions. These combinations are drawn in Figure 4.

It is emphasized that (1) and Figures 2–4 (essentially, $\mathcal{V}$, $\mathcal{H}$, and $\mathcal{M}$) apply identically to the imaginary anterior segment of an intact mandible *and* to an actual fractured-off section, but that is where the similarity ends. The physical manifestations of $\mathcal{V}$, $\mathcal{H}$, and $\mathcal{M}$ in the two scenarios are fundamentally distinct. They are not interchangeable. In the intact mandible, the system that is equivalent to $\mathcal{V}$, $\mathcal{H}$, and $\mathcal{M}$ is produced by the stresses within the bone. In the plated mandible, it is produced by the loads in the plates and by contact between the fractured bone surfaces. The demonstration of this critical difference constitutes a result of this study.

*2.1. Intact Mandible.* Elementary engineering beam theory is used to determine the stress systems (Figure 5) that are equivalent to a specific set of $+\mathcal{V}$, $\pm\mathcal{H}$, and $\pm\mathcal{M}$ (Figure 4). (The identical engineering principles are implicitly behind the generally accepted as "obvious" Figure 1 stresses.) A uniform compression is the equivalent to an anteriorly directed $\mathcal{H}$ ($c_{\mathcal{H}}$ in Figures 5(a), 5(b), and 5(c)). Similarly, uniform tensile stress, $t_{\mathcal{H}}$, is the equivalent to the posteriorly directed $\mathcal{H}$ in Figure 5(e). (There is no uniform tension or compression associated with $\mathbf{T}_3$, Figure 5(d), because $\mathbf{T}_3$, being vertical, requires that $\mathcal{H} = 0$ for equilibrium.) The equivalents of a cw $\mathcal{M}$ (Figure 5(b)) and a ccw $\mathcal{M}$ (Figures 5(c), 5(d), and 5(e)) are stress gradients with compression-on-top/tension-on-bottom ($c_{\mathcal{M}}$ on top/$t_{\mathcal{M}}$ on bottom) and the opposite, respectively. (A uniform stress, without a gradient, is sufficient for $\mathbf{T}_0$ equilibrium, Figure 5(a).) For completeness, the shear stress equivalent of $\mathcal{V}$ is included in Figure 5, but as generally done in the literature, it is henceforth ignored.

*2.2. Plated Mandible.* As noted above, Figures 2–4 and (1) also apply exactly to a plated fractured mandible (Figure 6(a)). However, the system that is equivalent to a specific set of $+\mathcal{V}$, $\pm\mathcal{H}$, and $\pm\mathcal{M}$ (Figure 4) is provided by the loads ($H_U$, $V_U$, $M_U$, $H_L$, $V_L$, $M_L$, $\mathcal{H}'$, and $\mathcal{V}'$) identified in the FBD of the plated fractured segment in Figure 6(b) not the distributed bone stresses at the imaginary section (Figures 1 and 5).

$H_{(\,)}$, $V_{(\,)}$, and $M_{(\,)}$ are the unknown forces and moments acting within the upper and lower plates directly overlying the bone fracture, Figure 6(b). $\mathcal{H}'$ and $\mathcal{V}'$ are representative of the normal (perpendicular) and shear contact forces, respectively, on the fractured bone surface if the two segments touch. (According to basic friction theory, the maximum $\mathcal{V}'$, $\mathcal{V}'_{\max} = \mu\mathcal{H}'$, where $\mu$ is the coefficient of friction between bones. This is likely to influence the results of experimental studies in which the mandible analogue plastic has a different $\mu$ than bone.)

Similar to the derivation of (1), three independent simultaneous equations of static equilibrium, based on the FBD in Figure 6(b), can be obtained by summing forces

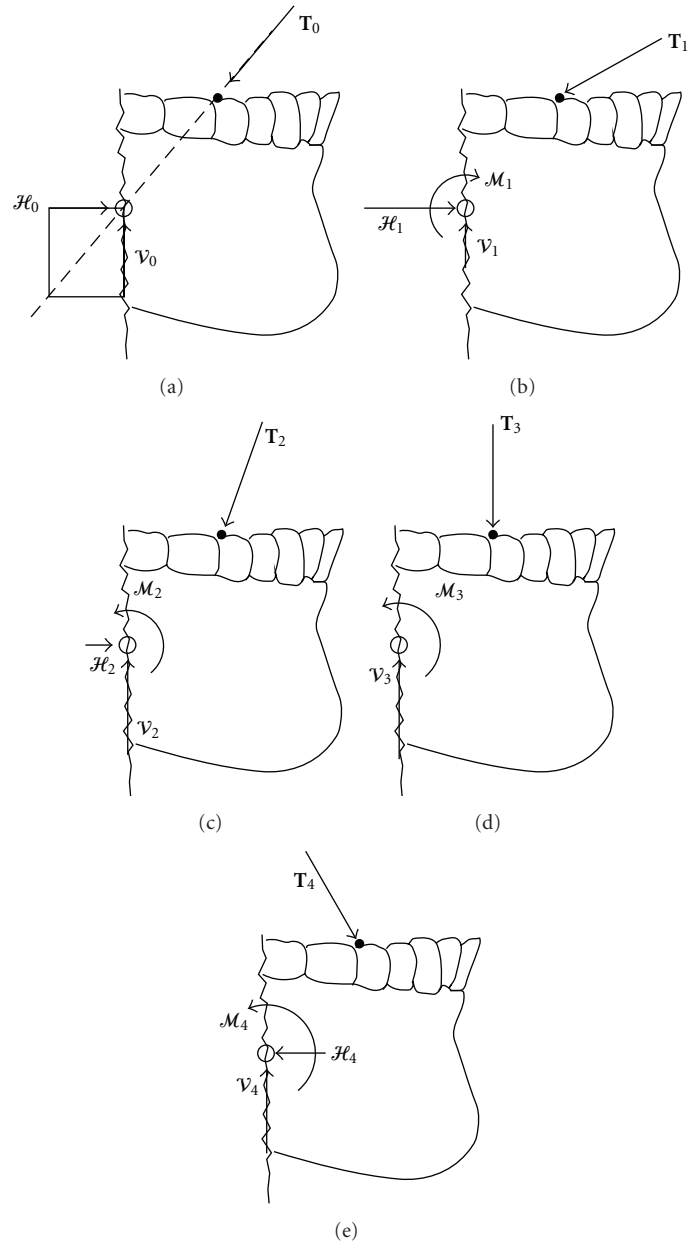


Figure 4: The internal forces ($\mathcal{V}$ and $\mathcal{H}$) and moment ($\mathcal{M}$) that are necessary for equilibrium with: (a) $\mathbf{T}_0$; (b) $\mathbf{T}_1$; (c) $\mathbf{T}_2$; (d) $\mathbf{T}_3$; (e) $\mathbf{T}_4$. (This figure applies to the intact and fractured anterior segment.)

in the vertical (2) and horizontal (3) directions and by summing moments (4) about the tooth contact point

$$-T_y + \mathcal{V}' + \mathrm{V_U} + \mathrm{V_L} = 0, \tag{2}$$

$$-T_x + \mathcal{H}' - \mathrm{H_U} - \mathrm{H_L} = 0, \tag{3}$$

$$g\mathcal{H}' - h\mathcal{V}' - \mathrm{d_U H_U} - h\mathrm{V_U} + \mathrm{M_U} - \mathrm{d_L H_L} - h\mathrm{V_L} + \mathrm{M_L} = 0. \tag{4}$$

Because there are fewer independent equations than unknown forces and moments (only $T_x$ and $T_y$ are known), this (statically indeterminate) problem cannot be solved using only the principles of static equilibrium. Fortunately, solving the problem is not a goal. Equations (2)–(4) serve as explicit evidence of the complexity of plating biomechanics.

## 3. Results

As consequence of LOA position (Figure 3), $\mathbf{T}_1$ produces a counterclockwise (ccw) moment (rotation) about the circle; $\mathbf{T}_0$ does not cause a rotation; $\mathbf{T}_2$, $\mathbf{T}_3$, and $\mathbf{T}_4$ produce clockwise (cw) rotations. For the equilibrium of the intact or fractured mandible, these moments, and $\mathbf{T}$'s horizontal and vertical components, must be opposed by the internal loads $\mathcal{M}$, $\mathcal{H}$, and $\mathcal{V}$, respectively, Figures 2(b) and 4 and (1).

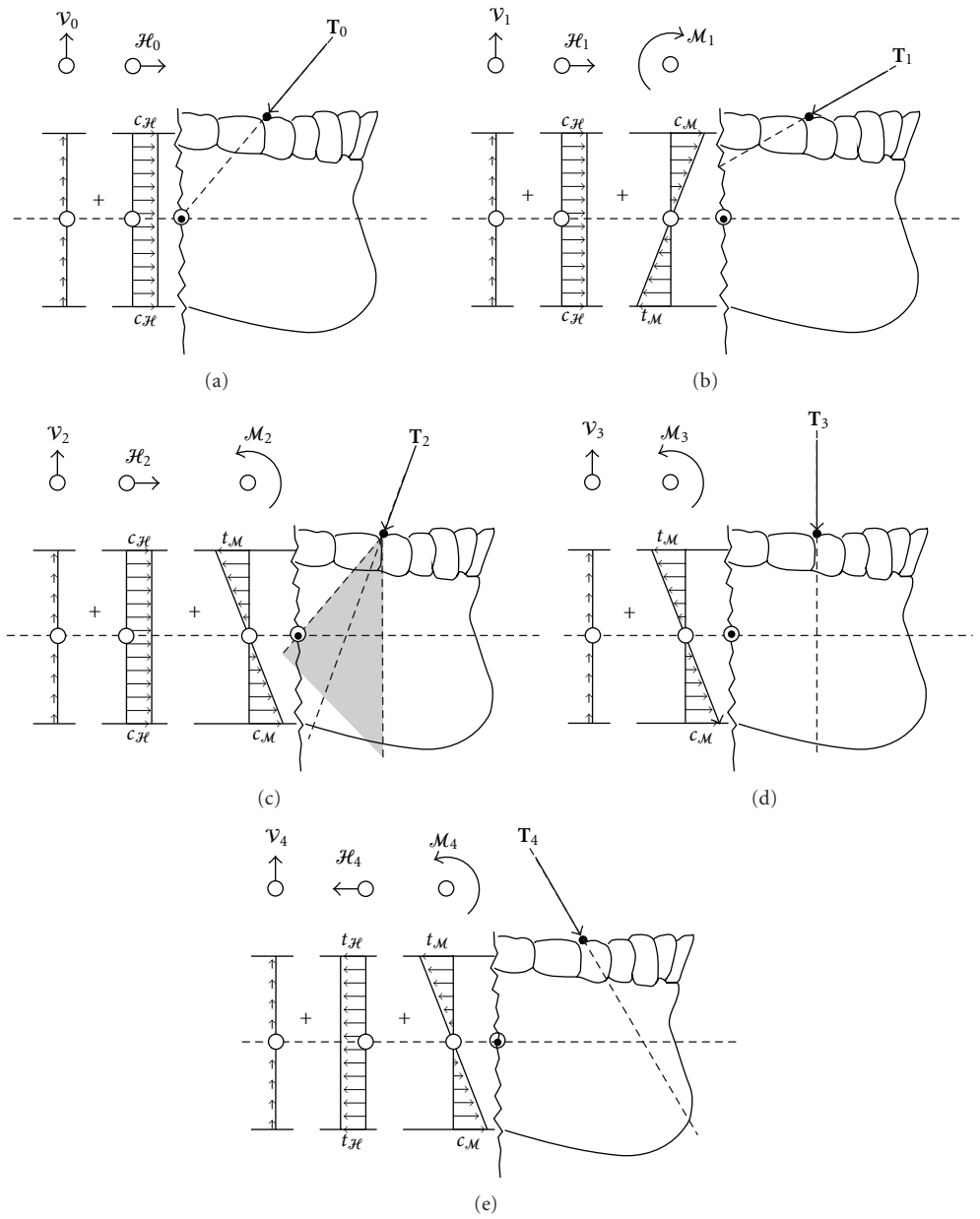


Figure 5: The tension, $t$, and compression, $c$, bone-stress distributions (not to scale) equivalent to $\mathcal{V}$, $\mathcal{H}$, and $\mathcal{M}$ (presented in Figure 4) for (a) $\mathbf{T}_0$; (b) $\mathbf{T}_1$; (c) $\mathbf{T}_2$; (d) $\mathbf{T}_3$; (e) $\mathbf{T}_4$. The shaded area in (c) indicates that the LOA of $\mathbf{T}_2$ falls between the LOAs of $\mathbf{T}_0$ and $\mathbf{T}_3$. (These figures are only relevant to the intact mandible.)

*3.1. Intact Mandible.* In the intact mandible, $\mathcal{V}$, $\mathcal{H}$, and $\mathcal{M}$ are expressed as equivalent stress distributions, Figure 5. The sums, according to the *superposition principle*, of those individual stress distributions (excluding the $\mathcal{V}$-associated shear stress) yield the net longitudinal tension/compression stress gradients shown in Figure 7. (The result in Figure 7(d) is identical to that depicted in Figure 1(a).)

*3.2. Plated Mandible.* In a plated mandible, the load system that is equivalent to $\mathcal{V}$, $\mathcal{H}$ and $\mathcal{M}$ is supplied by the loads on the plates and by the contacts between bone fragments. But even a simplified plated assembly (Figure 6) is far too intricate to solve with the methods of basic static equilibrium. Equations (1)–(4) clearly indicate the complex relationships between what is known/given and what is unknown.

## 4. Discussion

Three-dimensional (3D) numerical [26, 27] and experimental [28] models often lead to questions about the prevailing lever-based (tot/cob) stress distribution dogma. However, those previous criticisms involve the location of occlusal forces; the focus of this paper is on the direction

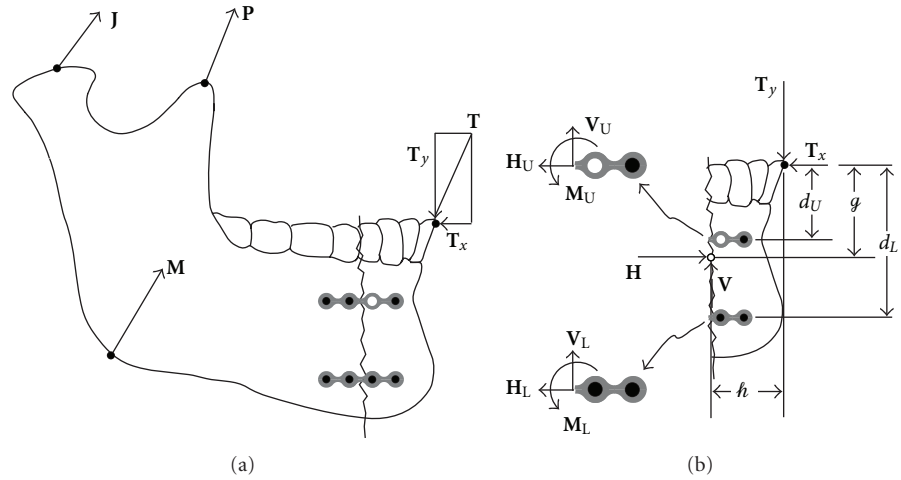


Figure 6: (a) Simplified FBD of a double plated mandible. (b) FBD of the anterior segment.

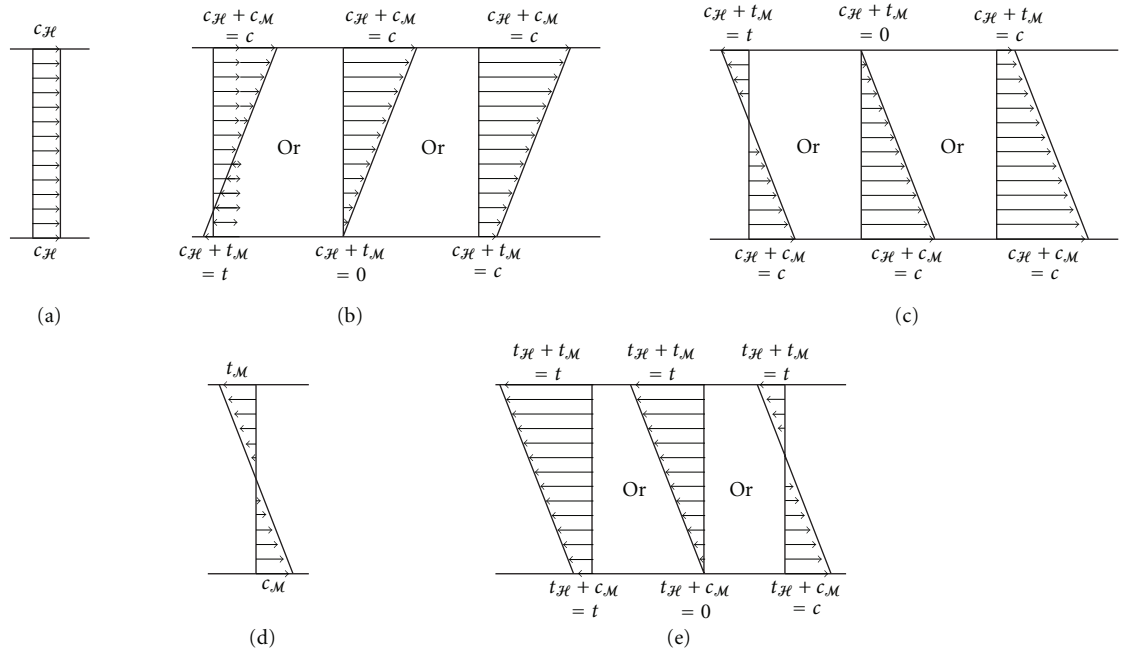


Figure 7: The (not to scale) sum of the longitudinal stress distributions (according to the *superposition principle*) of the $\mathcal{H}$ and $\mathcal{M}$ associated stresses presented in Figure 5 required for the equilibrium of the anterior segment when subjected to (a) $\mathbf{T}_0$; (b) $\mathbf{T}_1$; (c) $\mathbf{T}_2$; (d) $\mathbf{T}_3$; (e) $\mathbf{T}_4$. For illustrative purposes, the left side of Figure 7(b) is the actual sum of the longitudinal stress arrows in Figure 5(b), obtained by placing the stress arrows head-to-tail. Besides the lever (d), tot/cob is present only in (c)-left and (e)-right. (This figure applies only to the intact mandible.)

of those forces. Specifically, the lever-based two-dimensional (2D) model, Figure 1, consists of one force component direction (vertical) and one moment component direction (perpendicular to the page by the right-hand rule). The model in Figure 2, the basis for the presented analysis, adds the horizontal force component. This is the most general 2D model that is possible, and it is used to demonstrate serious deficiencies in the lever method without having to resort to the complexities of a 3D approach.

For convenience, and/or perhaps because of the lever model legacy, studies have generally been limited to occlusal forces in one (usually vertical, $\mathbf{T}_3$) direction. (In some experimental setups, the occlusal plane is slightly canted, so with a vertical force, the effect is similar to $\mathbf{T}_4$.) But there is no reason to believe that a bolus of food would necessarily elicit a vertical, or any particular, occlusal force direction. If, instead, crown-crown contact is assumed, then the vertical force assumption restricts analyses solely to frictionless flat-plane or edge-to-edge occlusions. This study is framed in the context of crown-crown contacts, so the specified contact angle (i.e., cusp incline angulation or incisal guidance) generally defines a nonvertical orientation

of the occlusal force. Some readers may prefer to attribute nonvertical occlusal forces to the interactions of muscle activity with the presence of a bolus of food. In either case, there is no compelling justification for the vertical occlusal force simplification, and as demonstrated, occlusal force direction is a critical determinant of the mechanical environment, $\mathcal{V}$, $\mathcal{H}$, and $\mathcal{M}$, within a mandible.

The FBD in Figure 3(b) can serve the same purpose as the FBD in Figure 2(b). However, the former is presented to emphasize that without the (entirely superfluous) mandible outline, this is actually a mundane static equilibrium problem in which a force, **T**, is being applied at a point located in a specified (by $g$ and $h$) position relative to another point, ◯, where the reactions $\mathcal{V}$, $\mathcal{H}$ and $\mathcal{M}$ are of interest. Therefore, for this aspect of the analysis, the only things that matter are the direction of **T**'s LOA and its position relative to (i.e., distance from) ◯. For specific quantitative values of $\mathcal{V}$, $\mathcal{H}$, and $\mathcal{M}$, the magnitude of **T** would also be needed. But for the qualitative analysis, the *relative* magnitudes of $\mathcal{V}$, $\mathcal{H}$, and $\mathcal{M}$ are sufficient, and because this is a linear model, these *relative* magnitudes do not change with changes in **T** magnitude. Another purpose for presenting Figure 3(b) as an alternative is to illustrate that the human mandible drawing in Figure 2(b) could easily be replaced with a nonhuman mandible, a machine part, and so forth. without any effects on $\mathcal{V}$, $\mathcal{H}$, and $\mathcal{M}$.

The 5 occlusal forces, $\mathbf{T}_{0--4}$, can cover the range of physiologically possible directions. But instead of a continuum of directions, it is more practical to consider categories of force directions defined by the positions of their LOA's relative to ◯, combined with the directions of their horizontal components. For example, whenever the LOA of a force passes through ◯, generically represented by $\mathbf{T}_0$, the results presented herein for $\mathbf{T}_0$ apply. Naturally, the angulation of $\mathbf{T}_0$ (defined by $g$ and $h$) would be different for incisal versus molar contact, nonetheless, qualitatively, the stress distributions would be identical. This concept is already being taken for granted with $\mathbf{T}_3$, because the stress distribution in Figure 1 is not specified for any particular contact location. $\mathbf{T}_2$'s LOA is bounded by $\mathbf{T}_3$ and $\mathbf{T}_0$, shaded region in Figure 5(c), so the associated stress distribution can be seen to morph, left to right in Figure 7(c), from the tot/cob of $\mathbf{T}_3$ (Figure 7(d)) to the complete compression of $\mathbf{T}_0$, (Figure 7(a)). Similar trends, but with less defined endpoints, occur with $\mathbf{T}_1$ and $\mathbf{T}_4$ because their LOA's are bound only on one side by $\mathbf{T}_0$ and $\mathbf{T}_3$, respectively.

*4.1. Intact Mandible.* The stress distribution within the body of the mandible is usually presented as in Figure 1. In the top part, there is a decreasing tension gradient from the gingival height, and near the mid-level, there is a reversal to an increasing gradient of compression toward the inferior border. This tension on top compression on bottom (tot/cob) stress distribution is consistent with the inherent vertical occlusal force of the lever. But in reality, in general, there must also be a nonzero horizontal bite force component, Figure 3, whenever inclined planes (cusps) contact each other. And as demonstrated, its presence has the potential to profoundly alter the stress distribution within the mandible from the generally accepted tot/cob (Figures 1, 5(d), and 7(d)) to, as an example, exactly the opposite (Figure 7(b), left).

The depictions of the relative magnitudes of the stress distributions in Figures 5 and 7 are not drawn to scale because the mathematical complexities of the governing equations, necessary for quantitative results, are being circumvented and because such detail would be unnecessarily obfuscating. Serendipitously, the simplifications are perfectly suited to the mathematics-minimized approach of this paper, because the critical nuances of Figure 7 can be examined without resorting to rigorous mathematics.

If **T** acts through the circle, $\mathbf{T}_0$, then the longitudinal stress in the body of the mandible is entirely a uniform compression, Figures 5(a) and 7(a). (As illustrated in Figure 4(a), $\mathbf{T}_0$ requires that $\mathcal{M} = 0$ for equilibrium, hence the uniform stress.) That, of course, is contrary to the tot/cob lever-based stress distribution, Figures 1 and 7(d).

The sums of the $\mathcal{H}_1$ associated uniform compression ($c_{\mathcal{H}}$) and the cw $\mathcal{M}_1$ associated $c_{\mathcal{M}} \rightarrow t_{\mathcal{M}}$ gradients of $\mathbf{T}_1$, Figures 4(b) and 5(b), can combine to produce 3 different net stress distribution patterns, Figure 7(b). Because both $\mathcal{H}_1$ and $\mathcal{M}_1$ are associated with compression in the top part of the mandible ($c_{\mathcal{H}}$ and $c_{\mathcal{M}}$, respectively), there is no doubt that the top part will be in compression. In the bottom part of the mandible, $\mathcal{H}_1$ is associated with compression ($c_{\mathcal{H}}$), but $\mathcal{M}_1$ is associated with tension ($t_{\mathcal{M}}$). Thus, depending on the relative magnitudes of $c_{\mathcal{H}}$ and $t_{\mathcal{M}}$, the net longitudinal stress in the bottom part of the mandible can be tensile, zero or compressive (left, middle, and right, respectively, in Figure 7(b)). To determine which of the three stress patterns reflects the actual stress, the governing beam equations would have to be solved. But for the present purposes, it suffices simply to note that all 3 potential $\mathbf{T}_1$ results are at variance with the lever's tot/cob stress distribution.

$\mathbf{T}_2$ (Figures 4(c) and 5(c)), like $\mathbf{T}_1$, produces a uniform compression consistent with $\mathcal{H}_2$, but because $\mathcal{M}_2$ is ccw, its associated gradient is $t_{\mathcal{M}} \rightarrow c_{\mathcal{M}}$. So, when these 2 longitudinal stress distributions are superimposed, Figure 7(c), it is certain that the bottom part of the mandible is in compression, but depending on the position of $\mathbf{T}_2$'s LOA within the shaded region in Figure 5(c), the top part can be in tension, stress-free, or in compression. More specifically, as $\mathbf{T}_2$ approaches vertical, its longitudinal stress distribution (Figure 7(c), left) looks more-and-more like the (vertical) $\mathbf{T}_3$-associated stress (Figure 7(d)). As $\mathbf{T}_2$'s direction approaches $\mathbf{T}_0$, its stress distribution, Figure 7(c) right, starts to resemble the $\mathbf{T}_0$ produced stress, Figure 7(a).

$\mathbf{T}_3$ (the lever replica, Figures 4(d) and 5(d)) is vertical, so there is no $\mathcal{H}_3$ equivalent stress. Its tot/cob stress distribution, Figures 1 and 7(d), is entirely the equivalent of the ccw $\mathcal{M}_3$. And finally, $\mathbf{T}_4$ (Figures 4(e) and 5(e)) is different from the others, because the $\mathcal{H}_4$ equivalent stress is a uniform tension. Combined with the ccw $\mathcal{M}_4$'s $t_{\mathcal{M}} \rightarrow c_{\mathcal{M}}$ gradient, the top portion of the mandible will be in tension, but the bottom portion can be in tension, stress-free, or in compression, Figure 7(e). Thus, of the 11 possibilities depicted in Figure 7, only 3 (left in Figure 7(c), Figure 7(d), and right in Figure 7(e)) are in concert with the lever's

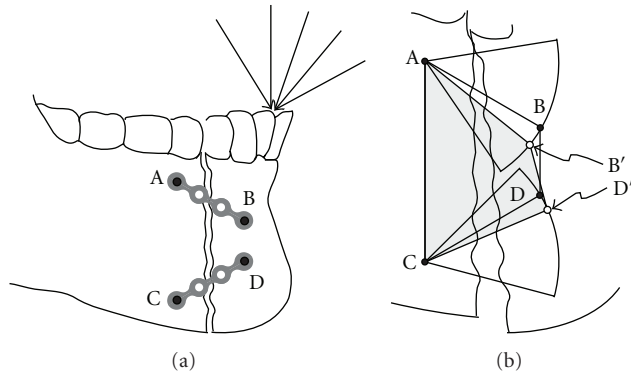


FIGURE 8: (a) Schematic representation of a fracture repair that forms a trapezoidal 4-bar linkage, ABDC. (b) The plate-constrained displacement, BD → B′D′, of the anterior segment.

tot/cob longitudinal stress distribution. The other 8 scenarios are contrary.

(Oral surgeons are intimately familiar with the biomechanical principles at work here. During extraction, the tooth can be considered as a vertical analogy to the mandible that is loaded as in Figures 5(b) and 5(c). When the tooth is luxated back and forth, $\pm\mathcal{M}$ are generated, and to reduce the associated tensile longitudinal stress in the root, a compressive (intrusive) force is applied concurrently, thereby reducing or eliminating the tension, analogous to the right sides of Figures 7(b) and 7(c) turned 90 degrees. A lever model of extraction would not account for the critical intrusive force component ($-\mathcal{H}$) that prevents tension-induced root fracture.)

*4.2. Plated Mandible.* For the plated mandible, Figure 6(b), there are an insufficient number of equations to solve for all unknowns. This statically indeterminate problem can be numerically modeled, typically with FEA [29–36], but whatever the solution may be, it must satisfy (2)–(4). Thus, as evidenced by the equations, everything is intertwined in a complex manner. Furthermore, if the fracture were at an angle, or if the plates were not horizontal or parallel, then (2)–(4) would be further complicated by trigonometric functions, different $h$ values for the upper and lower plates, and so on. This is clearly not a problem that is amenable to commonsensical analysis, especially with intuition that is based on the nonapplicable lever paradigm of the intact mandible.

Consider plates, AB and CD, secured with single screws at their ends, Figure 8(a). ABDC, Figure 8(b), forms a 4-bar linkage in which B and D are constrained to move along arcs of circles that are centered at A and C, respectively. Therefore, if for any reason B moves to B′, D must move to D′, because the bone dimension, BD (= B′D′), remains unchanged. Thus, with virtually any occlusal force, these plate constraints dictate a downward displacement with a ccw rotation of the anterior segment from BD to B′D′, hence the inferior border distraction. When the concepts and terminology from the intact mandible are applied to this outcome, it is ascribed to compression on top and tension on the bottom [26, 37]. But, in fact, the top plate, AB′, is in tension and CD′, the bottom plate, is in compression, and except for the compression at the bone-bone contact on top, there is no tension (which would be impossible anyway at a fracture) or compression in bone anywhere along the fracture. Thus, contrary to popular notion, the enlarged gap at the inferior border is not caused by tension; on the contrary, it is caused by compression in CD′.

There are, of course, many other 4-bar linkage configurations that would produce different interfragmentary displacements. Because plate AB, as the example, is secured by single screws at its ends, it can only transmit pure compression or tension—it is a 2-force member. (If, in Figure 6, the top plate was affixed with single screws at both ends, then $H_U \neq 0$, but $V_U = M_U = 0$.) Accounting for friction (between bone/plate or screw/plate), or even just one additional screw, would immensely complicate the problem by necessitating the inclusion of the shear forces (i.e., $V_U \neq 0$ in Figure 6(b)) and the bending moments (i.e., $M_U \neq 0$ in Figure 6(b)) in the plates. The relative bone movements would then depend mostly on plate deformations caused by those forces and moments. These complex statically indeterminate problems are typically solved with FEA. Clinically, however, it would be advantageous to conceptualize plate-imposed constraints in terms of linkages rather than the intact mandible paradigm. (Neither is realistic, but in this context, the intact idealization is entirely irrelevant and misleading.)

Although the focus is on plates, similar discussions would pertain to other modes of fixation. For example, in a sagittal split osteotomy, the transverse shear stresses within the bicortical screws and bone-bone friction produce the $\mathcal{V}$, $\mathcal{H}$, and $\mathcal{M}$ equivalent system. As with plating, the intact mandible mechanical environment is not applicable.

A mandible in function, intact or plated, is a complicated 3D statically indeterminate structure that is subjected to the complex interactions of variable anatomy and highly changeable muscle and occlusal forces. And, for many reasons, obvious and subtle, a plated fractured mandible is an entirely different and more complex load bearing structure than an intact mandible. If for no reason other than the impossibility of tensile stresses acting across a break, the tot/cob stress distributions illustrated in Figures 1, 5, and 7 are not possible at, or near, a fracture. According

to Saint Venant's principle, these stress distributions can be present only at some distance away from plated areas. Nevertheless, the Figure 1 tot/cob representations are often invoked explicitly [18, 20, 22, 23, 31] or implicitly in matters of fracture repairs.

Although the demonstrated analytical method is inadequate for the solution of these problems, it is the best instructional approach, and it is conceptually far more realistic than the ubiquitous lever model. This analysis is appropriate for conceptualizing mandibular biomechanics and for casting doubt on the status quo.

In conclusion, (1) the lever-based tension-on-top/compression-on-bottom (tot/cob) stress gradient should not be assumed in the intact mandible. It is only one of several possible stress distributions that depend on the direction of the occlusal force and the relative location of the section in question. (2) Internal forces ($\mathcal{H}$ and $\mathcal{V}$) and moment ($\mathcal{M}$) are necessary for the equilibrium of all mandibles, intact or fixed. Beyond sharing $\mathcal{H}$, $\mathcal{V}$, and $\mathcal{M}$, there are no valid comparisons between intact, plated, screwed, and so forth mandibles. (3) The stress distribution within an intact mandible should not be extrapolated to a plated, or otherwise stabilized, mandible.

## References


[1] W. L. Hylander, "The human mandible: lever or link?" *The American Journal of Physical Anthropology*, vol. 43, no. 2, pp. 227–242, 1975.

[2] W. L. Hylander, "Incisal bite force direction in humans and the functional significance of mammalian mandibular translation," *The American Journal of Physical Anthropology*, vol. 48, no. 1, pp. 1–7, 1978.

[3] J. W. Sikes Jr., B. R. Smith, and D. P. Mukherjee, "An in vitro study of the effect of bony buttressing on fixation strength of a fractured atrophic edentulous mandible model," *Journal of Oral and Maxillofacial Surgery*, vol. 58, no. 1, pp. 56–61, 2000.

[4] E. Ellis and G. S. Throckmorton, "Treatment of mandibular condylar process fractures: biological considerations," *Journal of Oral and Maxillofacial Surgery*, vol. 63, no. 1, pp. 115–134, 2005.

[5] G. P. Peterson, R. H. Haug, and J. Van Sickels, "A biomechanical evaluation of bilateral sagittal ramus osteotomy fixation techniques," *Journal of Oral and Maxillofacial Surgery*, vol. 63, no. 9, pp. 1317–1324, 2005.

[6] M. Karoglan, K. Schütz, H. Schieferstein, H. H. Horch, and A. Neff, "Development of a static and dynamic simulator for osteosyntheses of the mandible," *Technology and Health Care*, vol. 14, no. 4-5, pp. 449–455, 2006.

[7] M. J. Madsen and R. H. Haug, "A biomechanical comparison of 2 techniques for reconstructing atrophic edentulous mandible fractures," *Journal of Oral and Maxillofacial Surgery*, vol. 64, no. 3, pp. 457–465, 2006.

[8] A. E. Trivellato and L. A. Passeri, "Evaluation of osteotomy fixation changing the number, the extension and the location of the plates," *The British Journal of Oral and Maxillofacial Surgery*, vol. 44, no. 5, pp. 377–381, 2006.

[9] K. Ueki, D. Takazakura, K. Marukawa, M. Shimada, K. Nakagawa, and E. Yamamoto, "Relationship between the morphologies of the masseter muscle and the ramus and occlusal force in patients with mandibular prognathism," *Journal of Oral and Maxillofacial Surgery*, vol. 64, no. 10, pp. 1480–1486, 2006.

[10] E. Puricelli, "A new technique for mandibular osteotomy," *Head and Face Medicine*, vol. 3, no. 1, article 15, 2007.

[11] K. Ueki, K. Nakagawa, and E. Yamamoto, "Bite force and maxillofacial morphology in patients with Duchenne-type muscular dystrophy," *Journal of Oral and Maxillofacial Surgery*, vol. 65, no. 1, pp. 34–39, 2007.

[12] M. T. C. Leung, T. C. K. Lee, A. B. M. Rabie, and R. W. K. Wong, "Use of miniscrews and miniplates in orthodontics," *Journal of Oral and Maxillofacial Surgery*, vol. 66, no. 7, pp. 1461–1466, 2008.

[13] P. Mehra and H. Murad, "Internal fixation of mandibular angle fractures: a comparison of 2 techniques," *Journal of Oral and Maxillofacial Surgery*, vol. 66, no. 11, pp. 2254–2260, 2008.

[14] S. Schireson and M. Robinson, "The nonsurgical temporomandibular joint syndrome," *Archives of Otolaryngology*, vol. 73, pp. 681–685, 1961.

[15] P. D. Gingerich, "The human mandible: lever, link, or both?" *The American Journal of Physical Anthropology*, vol. 51, no. 1, pp. 135–138, 1979.

[16] R. M. S. Taylor, "Nonlever action of the mandible," *The American Journal of Physical Anthropology*, vol. 70, no. 4, pp. 417–421, 1986.

[17] E. Ellis III and L. R. Walker, "Treatment of mandibular angle fractures using one noncompression miniplate," *Journal of Oral and Maxillofacial Surgery*, vol. 54, no. 7, pp. 864–871, 1996.

[18] M. R. Tucker and M. W. Ochs, "Basic concepts of rigid internal fixation: mechanical considerations and instrumentation overview," in *Rigid Fixation for Maxillofacial Surgery*, M. R. Tucker, B. C. Terry, R. P. White et al., Eds., p. 32, Lippincott, Philadelphia, Pa, USA, 1991.

[19] S. Baker, D. Dalrymple, and N. J. Betts, "Concepts and techniques of rigid fixation," in *Oral and Maxillofacial Trauma*, R. J. Fonseca, R. V. Walker, N. J. Betts et al., Eds., p. 1284, Saunders, Philadelphia, Pa, USA, 1997.

[20] A. J. L. Gear, E. Apasova, J. P. Schmitz, and W. Schubert, "Treatment modalities for mandibular angle fractures," *Journal of Oral and Maxillofacial Surgery*, vol. 63, no. 5, pp. 655–663, 2005.

[21] R. D. Marciani, E. R. Carlson, and T. W. Braun, "Trauma," in *Oral and Maxillofacial Surgery*, R. J. Fonseca, Ed., p. 144, Saunders, St. Louis, Mo, USA, 2009.

[22] M. Champy, J. P. Loddé, R. Schmitt, J. H. Jaeger, and D. Muster, "Mandibular osteosynthesis by miniature screwed plates via a buccal approach," *Journal of Maxillofacial Surgery*, vol. 6, pp. 14–21, 1978.

[23] B. W. Davies, J. P. Cedema, and B. Guyuron, "Noncompression unicortical miniplate osteosynthesis of mandibular fractures," *Annals of Plastic Surgery*, vol. 28, no. 5, pp. 414–419, 1992.

[24] T. R. Katona, "The effects of cusp and jaw morphology on the forces on teeth and the temporomandibular joint," *Journal of Oral Rehabilitation*, vol. 16, no. 2, pp. 211–219, 1989.

[25] T. R. Katona, "A mathematical analysis of the role of friction in occlusal trauma," *Journal of Prosthetic Dentistry*, vol. 86, no. 6, pp. 636–643, 2001.

[26] F. H. M. Kroon, M. Mathisson, J. R. Cordey, and B. A. Rahn, "The use of miniplates in mandibular fractures. An in vitro study," *Journal of Cranio-Maxillo-Facial Surgery*, vol. 19, no. 5, pp. 199–204, 1991.

[27] R. H. Rudderman and R. L. Mullen, "Biomechanics of the facial skeleton," *Clinics in Plastic Surgery*, vol. 19, no. 1, pp. 11–29, 1992.

[28] V. Shetty, D. McBrearty, M. Fourney, and A. A. Caputo, "Fracture line stability as a function of the internal fixation system: an in vitro comparison using a mandibular angle fracture model," *Journal of Oral and Maxillofacial Surgery*, vol. 53, no. 7, pp. 791–802, 1995.

[29] T. Cox, M. W. Kohn, and T. Impelluso, "Computerized analysis of resorbable polymer plates and screws for the rigid fixation of mandibular angle fractures," *Journal of Oral and Maxillofacial Surgery*, vol. 61, no. 4, pp. 481–487, 2003.

[30] W. D. Knoll, A. Gaida, and P. Maurer, "Analysis of mechanical stress in reconstruction plates for bridging mandibular angle defects," *Journal of Cranio-Maxillofacial Surgery*, vol. 34, no. 4, pp. 201–209, 2006.

[31] H. H. Korkmaz, "Evaluation of different miniplates in fixation of fractured human mandible with the finite element method," *Oral Surgery, Oral Medicine, Oral Pathology, Oral Radiology and Endodontology*, vol. 103, no. 6, pp. e1–e13, 2007.

[32] E. Puricelli, J. S. O. Fonseca, M. F. de Paris, and H. Sant'Anna, "Applied mechanics of the Puricelli osteotomy: a linear elastic analysis with the finite element method," *Head and Face Medicine*, vol. 3, no. 1, article 38, 2007.

[33] H. Arbag, H. H. Korkmaz, K. Ozturk, and Y. Uyar, "Comparative evaluation of different miniplates for internal fixation of mandible fractures using finite element analysis," *Journal of Oral and Maxillofacial Surgery*, vol. 66, no. 6, pp. 1225–1232, 2008.

[34] S. T. Lovald, T. Khraishi, J. Wagner, and B. Baack, "Mechanical design optimization of bioabsorbable fixation devices for bone fractures," *Journal of Craniofacial Surgery*, vol. 20, no. 2, pp. 389–398, 2009.

[35] S. Parascandolo, A. Spinzia, P. Piombino, and L. Califano, "Two load sharing plates fixation in mandibular condylar fractures: biomechanical basis," *Journal of Cranio-Maxillofacial Surgery*, vol. 38, no. 5, pp. 385–390, 2009.

[36] T. Sugiura, K. Yamamoto, K. Murakami et al., "Biomechanical analysis of miniplate osteosynthesis for fractures of the atrophic mandible," *Journal of Oral and Maxillofacial Surgery*, vol. 67, no. 11, pp. 2397–2403, 2009.

[37] J. Tams, J. P. Van Loon, B. Otten, and R. R. M. Bos, "A computer study of biodegradable plates for internal fixation of mandibular angle fractures," *Journal of Oral and Maxillofacial Surgery*, vol. 59, no. 4, pp. 404–407, 2001.